

1991

Evidence for a Frozen Bed, Byrd Glacier, Antarctica

John P. Scofield

James L. Fastook

Terence J. Hughes

University of Maine - Main, terry.hughes@maine.edu

Follow this and additional works at: https://digitalcommons.library.umaine.edu/ers_facpub



Part of the [Earth Sciences Commons](#)

Repository Citation

Scofield, John P.; Fastook, James L.; and Hughes, Terence J., "Evidence for a Frozen Bed, Byrd Glacier, Antarctica" (1991). *Earth Science Faculty Scholarship*. 32.

https://digitalcommons.library.umaine.edu/ers_facpub/32

This Article is brought to you for free and open access by DigitalCommons@UMaine. It has been accepted for inclusion in Earth Science Faculty Scholarship by an authorized administrator of DigitalCommons@UMaine. For more information, please contact um.library.technical.services@maine.edu.

Evidence for a Frozen Bed, Byrd Glacier, Antarctica

JOHN P. SCOFIELD

Sawyer Environmental Research Center, University of Maine, Orono

JAMES L. FASTOOK

Department of Computer Sciences and Institute for Quaternary Studies, University of Maine, Orono

TERENCE J. HUGHES

Department of Geological Sciences and Institute for Quaternary Studies, University of Maine, Orono

Ice thickness, computed within the fjord region of Byrd Glacier on the assumptions that Byrd Glacier is in mass-balance equilibrium and that ice velocity is entirely due to basal sliding, are on average 400 m less than measured ice thicknesses along a radio-echo profile. We consider four explanations for these differences: (1) active glacier ice is separated from a zone of stagnant ice near the base of the glacier by a shear zone at depth; (2) basal melting rates are some 8 m/yr; (3) internal shear occurs with no basal sliding in much of the region above the grounding zone; or (4) internal creep and basal sliding contribute to the flow velocity in varying proportions above the grounding zone. Large gradients of surface strain rate seem to invalidate the first explanation. Computed values of basal shear stress (140 to 200 kPa) provide insufficient frictional heat to melt the ice demanded by the second explanation. Both the third and fourth explanations were examined by making simplifying assumptions that prevented a truly quantitative evaluation of their merit. Nevertheless, there is no escaping the qualitative conclusion that internal shear contributes strongly to surface velocities measured on Byrd Glacier, as is postulated in both these explanations.

1. INTRODUCTION

Byrd Glacier is an outlet glacier that flows through a fjord in the Transantarctic Mountains (80°-81°S, 152°-164°E). Its catchment area and flux into the Ross Ice Shelf are approximately $9.0 \times 10^5 \text{ km}^2$ and $20.5 \text{ km}^3 \text{ yr}^{-1}$ respectively. Flow converges above the fjord, peaks across the grounding zone halfway through the fjord, and diverges below the grounding zone where flow enters the Ross Ice Shelf. Center line surface velocities [Brecher, 1982] of 600 m/yr at the fjord entrance ($x = 40 \text{ km}$ in Fig. 1) increase to 875 m/yr across the grounding zone and decrease to 750 m/a at the fjord exit.

Swihinbank [1964] reported the first surface velocity measurements across Byrd Glacier near the grounding zone, using both surface theodolite triangulation to implanted stakes and aerial photogrammetric triangulation to moving crevasses. Surface velocity and elevation measurements have now been extended over the entire glacier between the fjord walls, using these methods, and surface strain rate components have been computed [Hughes and Fastook, 1981; Brecher, 1982, 1986; Scofield, 1988]. The force balance on Byrd Glacier has been analyzed by Whillans *et al.* [1989]. Here, we report possible velocity variations with depth.

Hughes [1977], Rose [1979], Weertman and Birchfield [1982], and later workers have assumed that high surface velocities associated with outlet glaciers and ice streams are due primarily to basal sliding. By assuming that flow is due solely to basal sliding, and that mass balance is zero because ice surface elevations have not changed since 1960 [Brecher, 1982], we produced an ice thickness map for Byrd Glacier. Our "balance thickness" map of bed topography is reliable only if the basal sliding assumption is valid. We shall examine this assumption.

2. BALANCE THICKNESS

To determine balance ice thickness within the fjord region of Byrd Glacier, we determined the flux crossing the ground zone and used this value to determine the balance thickness at points upstream under the assumptions of zero mass balance and flow due entirely to basal sliding. The grounding zone (Figure 1) was identified from evidence in the work by Hughes and Fastook [1981] and by comparing radio-echo thickness profiles with surface elevation [Brecher, 1982], assuming the glacier is in hydrostatic equilibrium with seawater at its grounding line. At the grounding zone the basal shear stress approaches zero and little or no internal shear exists. Thus the columnar average velocity is very close to the measured surface velocity and, together with the known radio-echo thickness and the flowband width, the flux at the grounding zone can readily be determined. A flowband defined by ice streamlines and measured velocity vectors [Brecher, 1982], and encompassing the radio-echo flightline, was selected (see Figure 1). Using this central flowband, instead of the glacier width, has the added advantage of eliminating a fjord shape factor, because the central flowband has vertical sides.

The balance thickness at any point along a flowband can be found from the following relationship:

$$H_{i+1} W_{i+1} \bar{U}_{i+1} = H_i W_i \bar{U}_i + \dot{a} (x_{i+1} - x_i) (W_{i+1} + W_i) / 2 \quad (1)$$

where ice thickness H , mean horizontal ice velocity \bar{U} averaged over H , and flowband width W are evaluated at integral steps i and $i + 1$ along flowband length x from $i = 0$ at the grounding line, and \dot{a} is the net accumulation rate (positive) or ablation rate (negative) from step i to step $i + 1$, summed for both the surface and the bed.

During the 1978-1979 field season on Byrd Glacier, mass-balance stakes recorded surface ablation rates that increased from 0.1 m/yr at the fjord entrance to 0.3 m/yr at the fjord exit during the austral summer.

Copyright 1991 by the American Geophysical Union.

Paper number 91JB00839
0148-0227/91/91JB-00839\$05.00

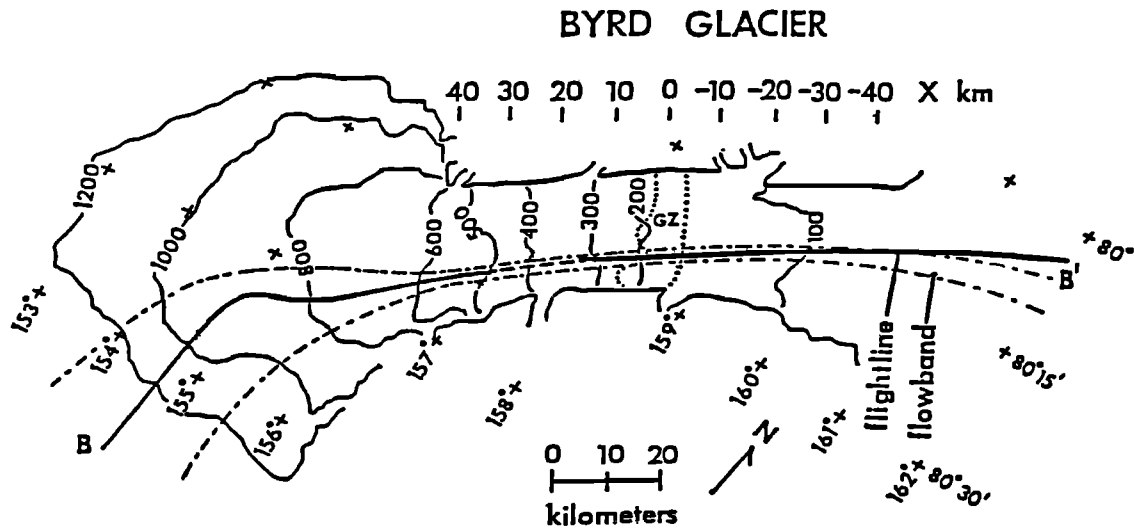


Fig. 1. Base map of the Byrd Glacier area. Flow is from left to right, the fjord entrance is located near $x = 40$ km. Mass-balance calculations were made along a flowband that includes radio-echo flightline B-B' in the half of Byrd Glacier fjord where ice is grounded. Note the coordinates for the x axis, and the location of the grounding zone (G.Z.), between transverse dotted lines. Data are absent for the dashed portions of the flightline.

Annual ablation rates can be estimated from the gradual transformation of the central glacier surface from large tabular blocks separated by a network of crevasses near the grounding line, halfway through the fjord, into isolated conical pinnacles rising from a relatively smooth surface near the fjord exist. Crevasses were initially narrow and about 20 m deep, but widened as ablation shrank and lowered the blocks over the 50 km to the fjord exit. A mean central ice velocity of 800 m/yr over this distance, along which ablation lowers the ice surface by some 20 m, gives an average surface ablation rate of about 0.3 m/yr.

There is no doubt that summer melting occurs on Byrd Glacier. *Swithinbank* [1964] described it, we observed meltwater pools on the wind-scalloped ice surface, and its extent is shown on Landsat imagery [Lucchitta and Ferguson, 1986]. Whether this meltwater evaporates or percolates into pores and cracks in the firm to refreeze, however, is an open question. Summer melting, runoff, and evaporation plus winter sublimation on Meserve Glacier (77.5°S, 162.3°E) cause about 0.3 m/yr of net ablation, ascribed primarily to dry katabatic winds [Bull and Carnein, 1970]. Dry katabatic winds are also strong on Byrd Glacier, so we can take 0.2 m/yr as an upper limit for the average net surface ice ablation upstream from the grounding line. Ice surface velocity averages about 740 m/yr in this 40 km distance, so surface ablation would reduce ice thickness less than 13 m if basal sliding dominates.

We estimate the total error on the resulting balance thicknesses to be about 15 percent. This includes a 2 percent error in measuring the flowband width, a 3 percent error in measuring surface velocity [Brecher, 1986], and a 5 percent error in ice thickness at the grounding line. For surface ice upstream from the grounding line, an uncertainty of -0.1 ± 0.1 m/yr in \dot{a} gives an uncertainty of ± 6.5 m in ice thickness.

When equation (1) is solved along a flowband = 2 km wide inside the fjord, which includes radio-echo profile B-B' (Figure 1) and allows for the slight departure of the flightline from measured flowlines, we find that the resulting balance thicknesses are on average 400 m less than the radio-echo thicknesses if \bar{U} is assumed to be the measured surface velocity U_M (Figure 2). Near the fjord entrance ($x = 40$ km) the difference is around 800 m. There are four explanations for the large discrepancy between the balance and radio-echo thicknesses: (1) basal sliding does not occur; instead, a shear zone at depth separates active ice above from stagnant ice near the base of the glacier; (2) basal sliding

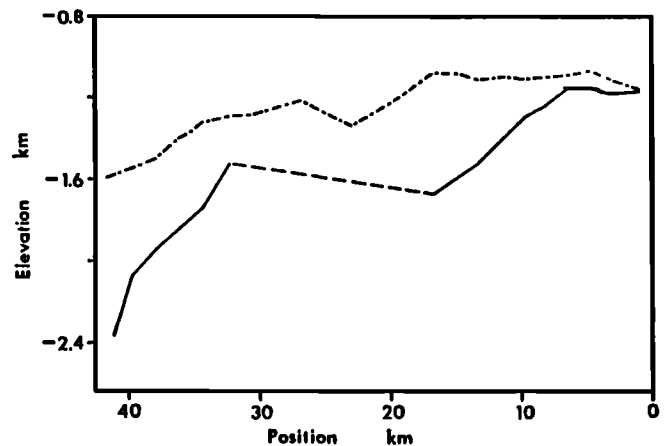


Fig. 2. Radio-echo bed (solid line), and bed assuming mass is conserved and flow is due entirely to basal sliding along B-B' (dot-dash line). The profiles extend from the fjord entrance ($x = 40$ km) to the grounding zone ($x = 0$) in Figure 1. The dashed portion of the radio-echo bed is the region where no bottom reflections were received. The difference between the two beds averages around 400 m. The largest discrepancy is around 800 m and occurs near the fjord entrance. Ice thicknesses along flightline B-B' were provided by the Scott Polar Research Institute.

occurs, but basal melt rates remove enough ice to conserve mass flux along the flowband; (3) the bed is frozen over most of the flowband, so that internal creep replaces basal sliding; and (4) internal creep dominates in some regions while basal sliding dominates in others. These hypotheses will now be examined.

3. SHEAR ZONE AT DEPTH

If our first hypothesis is correct, a narrow shear zone along profile B-B', shown by the dashed line in Figure 3, separates essentially "plug flow" above from essentially stagnant ice below. *Colbeck and Gow* [1979] have evidence of a situation similar to this in Greenland, although on a much smaller scale. They attribute the formation of a

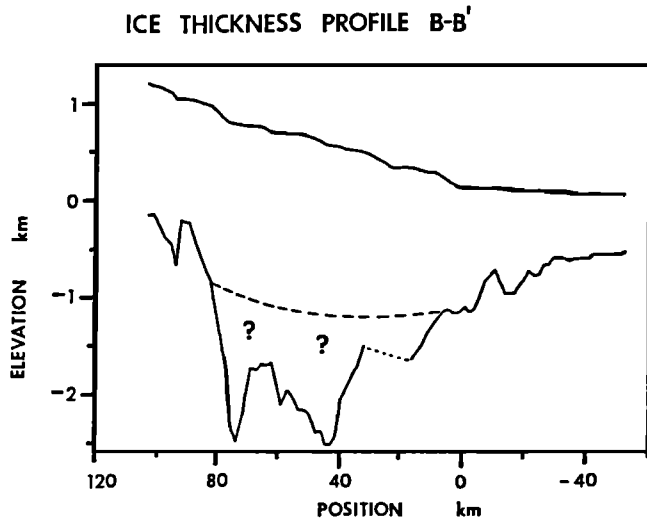


Fig. 3 Proposed dead ice zones superimposed on ice thickness profile B-B'. Long-dashed line is possible location of shear zone separating active ice above from dead ice below. Short-dashed line represents region where ice thickness is not known.

shear zone at depth to the concentration of shear strain rate in a narrow, horizontal band [Orowan, 1960] due to uphill flow along a grade of about 10 percent. Within Byrd Glacier fjord bedrock slopes of about 10 percent occur between $x = 5$ km and $x = 85$ km along flight line B-B' (Figure 3). It is possible that a band of high strain exists in this region, resulting in a concentrated, horizontal shear zone. However, although vertical shear zones along the sides of Byrd Glacier isolate stagnant bodies of ice in reentrant portions of the fjord walls, these shear zones are never less than 3 km wide. Hence, these lateral shear zones are as wide as or wider than Byrd Glacier is thick.

Longitudinal and transverse gradients in surface strain rates are even more compelling evidence that a smooth, narrow shear zone at depth does not exist. Brecher [1986] and Scofield [1988] measured longitudinal ($\dot{\epsilon}_{xx}$), transverse ($\dot{\epsilon}_{yy}$), and shear ($\dot{\epsilon}_{xy}$) surface strain rates throughout the fjord region. Gradients of $\dot{\epsilon}_{xx}$ and $\dot{\epsilon}_{yy}$ are consistent with flow that is influenced by bedrock topography [Scofield, 1988; Whillans et al., 1989]. The strain rates seem to indicate that basal ice flows around and over bedrock highs, and into bedrock lows, at least where these highs and lows are mapped along the radio-echo flightline in Figure 1. If a shear zone existed at depth, or for that matter if Byrd Glacier fjord had a flat bed, it is likely that $\dot{\epsilon}_{xx}$ would display gradual and continuous extension above the grounding zone, and $\dot{\epsilon}_{yy}$ would be determined only by flowband width.

4. HIGH BASAL MELT RATES

To determine an average basal melt rate necessary to preserve the grounding line flux along flightline B-B' under the assumption that flow is due solely to sliding on a melted bed, we fit straight lines to the radio-echo bed and the "balance thickness" sliding bed in Figure 2. From these, we calculated that a mean melt rate of around 8 ± 3 m/yr is necessary. Following Weertman [1963], we estimate that the maximum amount of strain heating available to melt ice at the base of Byrd Glacier is around 3.5×10^7 cal m^{-2} yr $^{-1}$ which is two orders of magnitude greater than the normal geothermal flux (C.R. Bentley, written communication, 1990), but still about an order of magnitude less than is necessary to maintain basal melt rates of 8 m/yr. This suggests that high basal melt rates cannot account for the differences between the radio-echo bed and the balance bed. Moreover, such a high basal

melting rate probably could not sustain the steep surface slope, because bed traction probably would be too low.

We conclude from these considerations, and from the low (< 0.2 m/yr) surface ablation rate in the fjord, that the term containing \dot{a} in equation (1) can be ignored because a negative mass balance would reduce ice thickness by less than 13 m behind the grounding line; this is within the uncertainty of the radio-echo ice thickness. The mean balance velocity \bar{U}_i averaged over depth at step i along B-B' in terms of velocity U_0 measured at the grounding line, where $i = 0$ and $U_0 = U_M$, is then obtained from equation (1) by setting $\dot{a} = 0$:

$$\bar{U}_i = \frac{H_0 W_0 U_0}{H_i W_i} \quad (2)$$

equation (2) will be used in the rest of this paper. Values of H_0 and H_i are from the radio-echo profile, and values of W_0 and W_i are taken from measured surface velocity vectors.

5. FROZEN BED

Balance velocities computed from equation (2) for basal sliding only are less than the measured surface velocities for all flowband cross sections for which $i > 0$. This suggests that internal creep accounts for a portion of the measured surface velocity, because creep velocity decreases with depth below the surface. If the bed is frozen, only creep occurs and a vertical profile of horizontal ice velocity can be computed for laminar flow in isothermal, homogeneous ice [Nye, 1952; Raymond, 1980; Hughes, 1981].

Taking the origin of coordinates at the grounding line, with x horizontal and positive upstream and z vertical and positive upward, shear stress σ_{xz} varies with depth $H - z$ through ice of thickness H as follows:

$$\sigma_{xz} = \rho g (H - z) \alpha \quad (3)$$

where ρ is ice density, g is gravity acceleration, and α is surface slope. The flow law of ice [Glen, 1955] for laminar flow is

$$\dot{\epsilon}_{xz} = (\sigma_{xz}/A)^n 1/2 [dU_c(z)/dz] \quad (4)$$

where $\dot{\epsilon}_{xz}$ is the shear strain rate, n is a viscoplastic exponent, A is a hardness parameter that is constant for isothermal homogeneous ice, and $U_c(z)$ is the creep velocity at height z above the bed.

Keeping flow law parameter A constant in equation (4), and integrating equation (4) using equation (3), gives the following relationship between creep velocity $U_c(z)$ at height z above the bed and average creep velocity $\bar{U}_c = \int_0^H [U_c(z)/H] dz$ in the ice column:

$$U_c(z) = \frac{(n+2) \bar{U}_c [H^{n+1} - (H-z)^{n+1}]}{(n+1) H^{n+1}} \quad (5)$$

For mass-balance equilibrium, $\bar{U}_c = \bar{U}_i$ in the flowband cross section at step i in equation (2), if the bed is frozen.

Let $U_c(z) = U_M$ at $z = H$, for which $(U_M)_i$ is the measured surface ice velocity at step i . Equation (5) at $z = H$ then becomes

$$\bar{U}_c = \left(\frac{n+1}{n+2} \right) U_M \quad (6)$$

When A is constant, the value of n has been reported to vary from 1.5 to 4.2 [Weertman, 1973]. For $n = 3$, the usual value, equation (6) gives an average velocity that is 80 percent of the measured surface velocity. If

the ratio of the balance velocity to the surface velocity is greater than 80 percent, then the measured velocity will have a sliding component U_S as well as a creep component U_C . For $n = 1.5$ and $n = 4.2$, the average velocity will be 71 percent and 84 percent of the measured surface velocity, respectively, if the bed is frozen.

Table 1 gives values of n in equation (6) for \bar{U} in equation (2) and U_M at various cross sections along profile B-B'. A high value of n approximates superplastic creep ($n = \infty$) and produces a velocity profile that is similar to one for $n = 3$ in which A decreases toward the bed as a result of thermal softening (in-creasing ice temperature), strain softening (developing an easy-glide ice fabric), or both, as postulated by Hughes [1977, Figure 23] for transverse shear on Byrd Glacier.

TABLE 1. Measured Surface Velocity U_M , Balance Velocity \bar{U} , the Ratio of the Balance Velocity to the Measured Surface Velocity in Percent (\bar{U}/U_M), and Viscoplastic Exponent n in Equation (6), Measured Along a 2.0- to 2.2-km-Wide Flowband That Includes Radio-Echo Flightline B-B'

x (km)	U_M (m s^{-1})	\bar{U} (m s^{-1})	\bar{U}/U_M (%)	n
.0	810	810	100	∞
1.1	805	791	98	48.0
2.9	805	766	95	18.0
4.5	810	756	93	12.3
6.1	772	740	96	23.0
7.6	741	678	92	10.5
9.6	715	632	88	6.3
11.2	715	589	82	3.5
13.0	702	548	78	2.5
14.7	704	516	73	1.7
16.5	697	497	71	1.4
32.0	563	497	88	6.3
34.0	548	446	82	3.6
35.8	522	425	82	3.6
37.5	495	406	82	3.6
39.3	478	383	80	3.0
41.1	460	329	72	1.6

For $n = 3$, a ratio \bar{U}/U_M less than 80 percent suggests that flow is due entirely to internal creep, and a ratio of 100 percent suggests that flow is due entirely to basal sliding.

In order that surface velocities calculated from equation (5) match the measured surface velocities, we solved equation (6) for n at each cross section (Table 1), and used this n in equation (5) to calculate the velocity profile for mass-balance equilibrium, $\bar{U}_C = \bar{U}_i$ in equation (2). The resulting profiles for a frozen bed at each cross section have the correct surface velocity, and conserve mass flux. Velocity profiles for selected cross sections are shown in Figure 4. These profiles require n to vary at each cross section along the flow-band while A remains constant, as listed in Table 1; or require a constant n , typically $n = 3$, while A decreases toward the bed at each cross section. Obvious weaknesses in this frozen-bed analysis are the assumptions of laminar flow and the wide variation of n or A that is required for measured surface velocities to be compatible with mass-balance velocities. The only remaining alternative is to allow variations in the ratio of creep to sliding velocities along the flowband. This requires a thawed-bed analysis.

6. THAWED BED

Computing vertical profiles of horizontal velocity without purely laminar flow makes use of measured surface strain rate components $\dot{\epsilon}_{ij}$ arising from the deviatoric stresses σ_{ij}' that are present, where subscripts ij denote axes x, y, z in the usual tensor notation. We will assume that Byrd Glacier has a linear temperature profile:

$$\theta(z) = \theta_B + (\theta_S - \theta_B)(z/H) \quad (7)$$

where θ is Celsius temperature, θ_S is the measured mean annual surface temperature, θ_B is the pressure melting temperature at the bed, and H is ice thickness in vertical direction z above the bed. We have approximated surface temperatures on the glacier by assuming that a surface temperature of -24°C exists at the 100-m elevation contour [Thomas, 1976] and that the adiabatic lapse rate in this region is -1°C per 100-m elevation gain, as was measured for Meserve Glacier [Hughes, 1971]. Temperature appears in hardness parameter A in the flow law of ice, which can be written two ways [Glen, 1958]:

$$\dot{\epsilon} = (\tau/A)^n \quad (8a)$$

$$\dot{\epsilon}_{ij} = (\tau^{n-1}/A^n) \sigma_{ij}' \quad (8b)$$

where $\dot{\epsilon}$ and τ are the effective strain rate and effective deviatoric stress, respectively. Solving equations (8) for σ_{ij}' results in the following:

$$\sigma_{ij}' = A \dot{\epsilon}^{n/(n-1)} \dot{\epsilon}_{ij} \quad (9)$$

Following Budd [1969, p. 25] and using equation (7):

$$\begin{aligned} A &= A_0 \exp(-C \theta_B) \exp[-C(\theta_S - \theta_B)z/H] \\ &= K \exp(-kz) \end{aligned} \quad (10)$$

where $C \approx 0.03^\circ\text{C}^{-1}$ for $n = 3$, A_0 is constant if ice fabric, density, and purity do not vary significantly with depth through Byrd Glacier, $k = C(\theta_S - \theta_B)/H$, and $K = A_0 \exp(-C \theta_B)$.

Vertical velocity profiles can be obtained by numerically computing the downstream velocity at each dz step i , from $i = 0$ at the bed to $i = H/dz$ at the surface. For each dz step, the velocity change dU is obtained from equation (9) for $\dot{\epsilon}_{ij} = \dot{\epsilon}_{xz}$:

$$1/2 (dU/dz) = \dot{\epsilon}_{xz} = \dot{\epsilon}^{(n-1)/n} \sigma_{xz}/A \quad (11)$$

By definition:

$$\begin{aligned} \dot{\epsilon} &= [1/2 (\dot{\epsilon}_{xx}^2 + \dot{\epsilon}_y^2 + \dot{\epsilon}_{zz}^2 \\ &\quad + 2\dot{\epsilon}_{yx}^2 + 2\dot{\epsilon}_{yz}^2 + 2\dot{\epsilon}_{xz}^2)]^{1/2} \\ &\approx (\dot{\epsilon}_{xx}^2 + \dot{\epsilon}_y^2 + \dot{\epsilon}_{xx}\dot{\epsilon}_{yy} + \dot{\epsilon}_{xy}^2 + \dot{\epsilon}_{xz}^2)^{1/2} \end{aligned} \quad (12)$$

where $\dot{\epsilon}_{zz} = -(\dot{\epsilon}_{xx} + \dot{\epsilon}_{yy})$ for mass conservation and $\dot{\epsilon}_{yz}$ is assumed negligible throughout H for the flowband under consideration. Values of surface strain rate components $\dot{\epsilon}_{xx}$, $\dot{\epsilon}_{yy}$, and $\dot{\epsilon}_{xy}$ and basal shear stress τ_0 , where $\tau_0 = \sigma_{xz}$ at $z = 0$ in equation (3) along flightline B-B', are listed in Table 2. Given that shear stress σ_{xz} for constant ice density increases linearly with depth, from zero at the surface to a maximum at the bed, then strain rate component $\dot{\epsilon}_{xz}$ will only contribute significantly to $\dot{\epsilon}$ in equation (12) near the base of the glacier. Taking $n = 3$ and $A \approx 10^{-16} \text{ kPa}^{-3} \text{ s}^{-1}$ at -15°C [Paterson, 1981, p. 39, Table 3.3], and $\tau_0 = 200 \text{ kPa}$ near $x = 32 \text{ km}$ in Table 2, gives $\dot{\epsilon}_{xz} = 0.025 \text{ a}^{-1}$ in equation (4). Including this value of $\dot{\epsilon}_{xz}$ in equation (12) results in an effective strain rate of 0.036 yr^{-1} at the base of the glacier, assuming that $\dot{\epsilon}_{xx}$, $\dot{\epsilon}_{yy}$, and $\dot{\epsilon}_{xy}$ are constant with depth, whereas excluding $\dot{\epsilon}_{xz}$ results in an effective strain rate of 0.026 yr^{-1} . Upstream from $x = 32 \text{ km}$, τ_0 generally increases, so the difference between the two values of $\dot{\epsilon}$ tends to increase, whereas downstream from

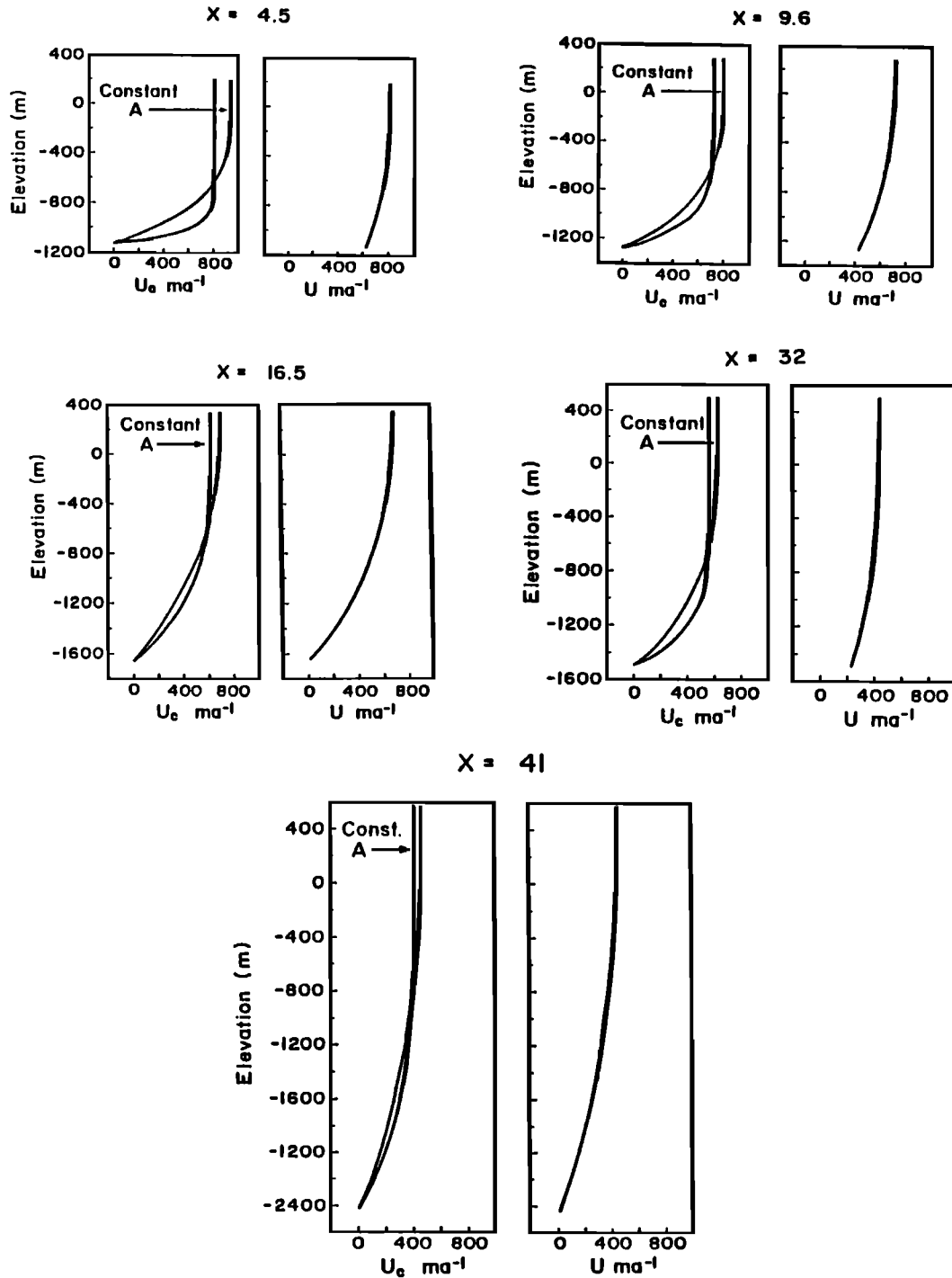


Fig. 4. Vertical velocity profiles computed for frozen (left) and thawed (right) beds at $x = 4.5, 9.6, 16.5, 32,$ and 41 km upstream from the grounding line. Velocity profiles for a frozen bed are shown for laminar flow in which the measured surface velocity is reproduced for variable A , but not for constant A , when $n = 3$. Velocity profiles for a thawed bed reproduce the measured surface velocity for variable A , constant effective strain rate, and a linear temperature profile, when $n = 3$.

$x = 32$ km, τ_0 tends to decrease, as do $\dot{\epsilon}_{xx}$, $\dot{\epsilon}_{yy}$, and $\dot{\epsilon}_{xy}$ (see Table 2). Over most of the region in question the difference between the two values is small enough so that $\dot{\epsilon}_{xz}$ can be ignored in calculating $\dot{\epsilon}$ from equation (12).

Assuming that components $\dot{\epsilon}_{xx}$, $\dot{\epsilon}_{yy}$, and $\dot{\epsilon}_{xy}$ combine such that $\dot{\epsilon}$ varies little with z , then equation (11) can be integrated for constant $\dot{\epsilon}$ and A_0 , by substituting for A and σ_{xz} from equations (10) and (3):

$$\begin{aligned}
 U_c - U_s &= \int_{U_s}^{U_c} du = \int_0^z 2\dot{\epsilon}_{xz} dz \\
 &= \left(2 \rho g A_0 \dot{\epsilon}^{-(n-1)/n} / K \right) \int_0^z (H - z) \exp(kz) dz \\
 &= U^* [(1 - zk + Hk) \exp(kz) - Hk - 1] \quad (13)
 \end{aligned}$$

TABLE 2. Longitudinal ($\dot{\epsilon}_{xx}$), Transverse ($\dot{\epsilon}_{yy}$), and Side Shear Strain Rate ($\dot{\epsilon}_{xy}$) at the Surface of the Glacier, and Basal Traction Stress (τ_o)

Along Flowband B-B'				
x (km)	$\dot{\epsilon}_{xx}$ (a ⁻¹)	$\dot{\epsilon}_{yy}$ (a ⁻¹)	$\dot{\epsilon}_{xy}$ (a ⁻¹)	τ_o (kPa)
1.1	0.001	0.000	0.004	93
2.9	0.000	0.001	0.004	95
4.5	0.001	0.003	0.005	107
6.1	0.001	0.005	0.006	121
7.6	0.008	0.008	0.008	132
9.6	0.010	0.010	0.010	155
11.2	0.003	0.005	0.012	150
13.0	0.005	0.000	0.015	145
14.7	0.008	-0.001	0.018	153
16.5	0.006	-0.001	0.021	159
32.0	0.006	-0.002	0.023	198
34.0	0.008	-0.003	0.024	220
35.8	0.007	-0.004	0.023	294
37.5	0.006	-0.008	0.022	307
39.3	0.005	-0.013	0.021	278
41.1	0.005	-0.010	0.020	296

The strain rates are from Scofield (1988) and the traction stresses are computed from equation (3) where the surface slope α is averaged over a distance of approximately 20 km.

where U^* is a velocity given by:

$$U^* = 2 \rho g A_o \dot{\epsilon}^{(n-1)h} / Kk^2 \quad (14)$$

Equation (13) can be solved for the variation of internal creep velocity U_c versus depth. So that mass flux is conserved, the basal sliding velocity U_s at each cross section is the difference between the balance velocity \bar{U} calculated in equation (2) and the columnar average creep velocity, \bar{U}_c . The value of A_o in equation (14) is allowed to vary until the sum of the sliding velocity and the creep velocity at the surface U_c (H) equals the measured surface velocity U_M at each cross section. Table 3 lists the variation of A_o , \bar{U} , \bar{U}_c , and U_s at cross sections where the ice thickness is known along profile B-B' between the grounding zone and $x = 41$ km. Values of A_o in Table 3 are 2 to 10 times smaller than those tabulated by Paterson [1981, page 39, Table 3.3]. This implies a complex state of stress in Byrd Glacier that produces substantial strain hardening, assuming our A_o values are real. The resulting velocity profiles from five of the cross sections are shown in Figure 4. While basal sliding generally increases toward the grounding line, these data

TABLE 3. Ice Thickness H, Balance Velocity \bar{U} , Average Creep Velocity \bar{U}_c , Basal Sliding Velocity U_s , and Value of A_o , Which Result From Velocity Profiles Along Flightline B-B' Constructed Using Our Fourth Model

x (km)	H (m)	\bar{U} (ma ⁻¹)	\bar{U}_c (ma ⁻¹)	U_s (ma ⁻¹)	(%) \bar{U}_c	$A_o(10^{-17}$ kPa ⁻³ s ⁻¹)
1.1	1286	791	32	759	4	5.1
2.9	1320	766	94	672	12	14.3
4.5	1318	756	123	633	16	11.9
6.1	1343	740	76	664	10	6.5
7.6	1463	678	149	529	22	6.7
9.6	1562	632	198	434	31	5.7
11.2	1668	589	305	176	52	11.5
13.0	1789	548	372	176	68	12.3
14.7	1890	516	451	65	87	11.5
16.5	1982	497	480	17	97	10.8
32.0	1996	497	160	225	32	2.5
34.0	2223	446	245	201	55	3.1
35.8	2332	425	238	187	56	2.2
37.5	2438	406	214	192	53	1.8
39.3	2580	383	230	153	60	2.0
41.1	2993	329	315	14	96	2.3

* percentage of the balance velocity due to creep at each position, % \bar{U}_c .

suggest that it is the dominant flow mechanism in only the last 10 km above the grounding zone. Variations of A_o along x in Table 3, if they are real, show that ice entering the fjord is very hard for the first 9 km, softens greatly for the next 5 km after a gap of 16 km in ice thickness data, hardens somewhat for the next 5 km, softens for the next 3 km, and hardens somewhat across a grounding zone about 3 km wide. This variation of A_o would imply adjustments of ice fabrics to accommodate various ratios of ϵ_{xx} to ϵ_{xz} as the proportion of basal sliding to internal shear changes. Very hard ice entering the fjord may have a random fabric inherited from a complex state of stress in ice converging on Byrd Glacier. Soft ice then develops where the basal sliding velocity U_s is low, which implies a preferred ice fabric produced by laminar flow. Ice hardens when U_s increases, perhaps due to re-crystallization into a multiple-maximum fabric. However, it is also possible that the calculated variations in A_o are not real, given uncertainties in velocity and thickness data.

7. CONCLUSIONS

Ice thicknesses computed for mass-balance equilibrium and an ice velocity due only to basal sliding tend to be much less than ice thicknesses measured along a radio-echo flightline. We rule out a narrow shear zone at depth and massive basal melting as explanations for this discrepancy. We cannot rule out a frozen bed or a thawed bed, above which ice creep rates vary with distance upstream from the grounding line. This variation is drastic above a frozen bed but is reduced by basal sliding on a thawed bed. To distinguish between these two probabilities, it will be necessary to produce an areal map of bed topography from a dense grid of radio-echo flightlines, and integrate bed topography with our areal maps of surface elevations, velocities, and strain rates, using a three-dimensional finite element model of ice stream dynamics that allows a patchwork of frozen and thawed areas on the bed.

Acknowledgments. We express our thanks to Henry Brecher for providing us with the velocity and surface elevation data, to Robert Bindschadler, Charles Bentley, and an anonymous reviewer for helpful reviews, and to Charles Swithinbank and David Drewry for providing us with radio-echo profile B-B'. This work was supported by NSF grants DPP77-22204 and DPP07918681.

REFERENCES

- Brecher, H.H., Photographic determination of surface velocities and elevations on Byrd Glacier, *Antarc. J.U.S.* 17 (5), 79-81, 1982.
- Brecher, H.H., Surface velocity determination on large polar glaciers by aerial photogrammetry, *Ann. Glaciol.*, 8, 22-26, 1986.
- Budd, W.F., The Dynamics of Ice Masses, *Aust. Nat. Antarct. Res. Exped. Interim Rep. Ser. A(IV)*, *Glaciol.*, 108 pp., 1969.
- Bull, C., and C.R. Comein, The mass balance of a cold glacier, Meserve Glacier, South Victoria Land, Antarctica. *IAHS, Publ. 86*, 429-446, 1970.
- Colbeck, S.C., and A.J. Gow, The margin of the Greenland Ice Sheet at ISUA, *J. Glaciol.*, 24 (90), 155-165, 1979.
- Glen, J.W., The creep of polycrystalline ice. *Proc. R. Soc. London, Ser. A* (228), 519-538, 1955.
- Glen, J.W., The flow law of ice. *IAHS, Publ. 47*, 171-183, 1958.
- Hughes, T., Structural glaciology of Meserve Glacier, Phase 3. *Antarc. J. U.S.*, 6 (4), 127-128, 1971.
- Hughes, T., West Antarctic ice streams. *Rev. Geophys.*, 15 (1), 1-46, 1977.
- Hughes, T.J. 1981. Numerical reconstructions of paleo ice sheets, in *The Last Great Ice Sheet*, edited by G. H. Denton and T. Hughes, pp. 221-261, Wiley-Interscience, New York, 1981.
- Hughes, T.J., and J.L. Fastook, Byrd Glacier: 1978-1979 field results. *Antarc. J. U.S.*, 16(5), 86-89, 1981.
- Lucchitta, B.K., and M. Ferguson, Antarctica: Measuring glacier velocity flow from satellite images, *Science*, 234, 1106, 1986.
- Nye, J.F., The mechanics of glacier flow. *J. Glaciol.*, 2 (12), 82-93, 1952.
- Orowan, E., Mechanism of seismic faulting. *Geol. Soc. Am. Bull.*, 79, 323-345, 1960.

- Paterson, W.S.B., *The Physics of Glaciers*, 2nd ed., 380 pp., Pergamon, New York, 1981.
- Raymond, C.F., Temperate valley glaciers, in *Dynamics of Snow and Ice Masses*, edited by S. C. Colbeck, pp. 79-139, Academic, San Diego, Calif., 1980.
- Rose, K.E., Characteristics of ice flow in Marie Byrd Land, Antarctica, *J. Glaciol.*, 24 (90), 63-75, 1979.
- Scofield, J.P., Flow Characteristics of an Outlet Glacier: Byrd Glacier, Antarctica, M.S. thesis, University of Maine, Orono, 1988.
- Swithinbank, C.W.M., To the valley glaciers that feed the Ross Ice Shelf, *Geograph. J.*, 130, 30-48, 1964.
- Thomas, R.H., The distribution of 10 m temperatures on the Ross Ice Shelf, *J. Glaciol.*, 16 (74), 111-117, 1976.
- Weertman, J., Profile and heat balance at the bottom surface of an ice sheet fringed by mountain ranges, *IAHS*, 61, 245-252, 1963.
- Weertman, J., Creep of ice, in *Physics and Chemistry of Ice*, edited by E. Whalley, S. J. Jones and L. W. Gold, pp. 320-337, Royal Society of Canada, Ottawa, 1973.
- Weertman, J., and G.E. Birchfield, Subglacial water flow under ice streams and West Antarctic ice sheet stability, *Ann. Glaciol.*, 3, 316-320, 1982.
- Whillans, I.M., Y.H. Chen, C.J. van der Veen, and T. Hughes, Force Budget III: Application to three-dimensional flow of Byrd Glacier, Antarctica, *J. Glaciol.*, 35 (119), 68-80, 1989.
-
- J.L. Fastook, Department of Computer Sciences and Institute for Quaternary Studies, University of Maine, Orono, ME 04469
- T.J. Hughes, Department of Geological Sciences and Institute for Quaternary Studies, University of Maine, Orono, ME 04469
- J.P. Scofield, Sawyer Environmental Research Center, University of Maine, Orono, ME 04469

(Received March 14, 1990;
revised January 30, 1991;
accepted March 8, 1991.)